Eur. Phys. J. C (2025) 85:1315
https://doi.org/10.1140/epjc/s10052-025-15054-4

THE EUROPEAN PHYSICAL JOURNAL C

Regular Article - Theoretical Physics

Quantum corrections to the thermodynamics of R-charged D1-branes

Behnam Pourhassan[1,a], **Saheb Soroushfar**[2,b], **Hoda Farahani**[1,c], **Mir Faizal**[3,4,5,d]

[1] School of Physics, Damghan University, 3671641167 Damghan, Iran
[2] Department of Physics, College of Sciences, Yasouj University, 75918-74934 Yasouj, Iran
[3] Department of Physics and Astronomy, University of Lethbridge, Lethbridge, AB T1K 3M4, Canada
[4] Irving K. Barber School of Arts and Sciences, University of British Columbia, Kelowna, BC V1V 1V7, Canada
[5] Canadian Quantum Research Center, 204-3002 32 Ave, Vernon, BC V1T 2L7, Canada

Received: 3 August 2025 / Accepted: 7 November 2025

Abstract We investigate the quantum thermodynamics of R-charged D1-branes by incorporating non-perturbative exponential corrections that arise naturally from D-instanton contributions in type IIB string theory. Our approach extends beyond classical supergravity solutions to capture the quantum gravitational regime where traditional thermodynamic descriptions break down. Through systematic analysis of the corrected entropy expression, we derive quantum-modified thermodynamic potentials including temperature, specific heat, internal energy, and Helmholtz free energy, revealing profound deviations from classical behavior in the small-horizon limit where quantum effects dominate. The exponential corrections induce thermodynamic instabilities characterized by negative specific heat and modify the brane's phase structure, while breaking fundamental scaling relations such as the Smarr formula through quantum deviations that encode the breakdown of classical symmetries. We extend our analysis to quantum work and thermodynamic geometry, demonstrating that these corrections reveal strong attractive microstructural interactions and potential phase transitions near extremality. The thermodynamic curvature diverges negatively in the quantum regime, signaling enhanced correlations among underlying degrees of freedom. Through the AdS/CFT correspondence, we interpret these bulk quantum effects within the dual (1 + 1)-dimensional supersymmetric Yang–Mills theory, identifying suppressed degrees of freedom, anomalous scaling behavior, and quantum-induced trace anomalies in the boundary stress tensor. Our holographic renormalization analysis reveals that quantum corrections effectively reduce the central charge and introduce conformal symmetry breaking, reflecting the deep influence of quantum gravity on strongly coupled gauge theories. These findings establish the critical importance of quantum corrections in black brane thermodynamics and provide new insights into the holographic structure of gauge theories under quantum gravitational influence.

Contents

[a] e-mail: b.pourhassan@du.ac.ir
[b] e-mail: soroush@yu.ac.ir (corresponding author)
[c] e-mail: h.farahani@umz.ac.ir
[d] e-mail: mirfaizalmir@googlemail.com

Published online: 17 November 2025

1 Introduction

The thermodynamics of black branes, particularly those arising from string theory constructions, has become a key area of investigation in understanding the connection between gravity, thermodynamics, and quantum theory [1–4]. Among these, R-charged black branes play an important role due to their rich structure and correspondence with supersymmetric Yang-Mills theories in lower dimensions [5–7]. In this work, we focus on the R-charged D1-brane, a solution in type IIB supergravity [8–10], which exhibits interesting thermodynamic behavior due to its near-horizon geometry and its coupling to a lower-dimensional gauge theory via holography in the presence of quantum corrections.

While classical analyses of black branes offer significant insights into their equilibrium thermodynamic properties, they remain incomplete when approaching regimes where quantum gravitational effects become non-negligible. In such domains, particularly near the Planck scale or in the ultraviolet limit of the theory, quantum corrections play a pivotal role in shaping the behavior and stability of the underlying geometry. These corrections emerge from both perturbative and non-perturbative sectors of quantum gravity, with contributions arising from loop effects, thermal fluctuations, and stringy or brane microstate dynamics [11,12].

A key consequence of these quantum effects is the modification of fundamental thermodynamic quantities such as entropy, temperature, specific heat, and free energy. For instance, the leading order quantum corrections to black hole entropy are often logarithmic in nature and can be derived from various approaches including loop quantum gravity, quantum geometry, and conformal field theory via Cardy-type formulae [13,14]. Beyond these, non-perturbative corrections–frequently modeled through exponential terms–capture deep aspects of the microstructure of spacetime and are especially significant in systems with holographic duals, such as D-branes and black branes in string theory [15,16].

These exponential corrections, which often appear as e^{-S_0} terms in the corrected entropy, reflect the contribution of rare quantum configurations and tunneling effects and are crucial in probing the non-equilibrium behavior of black objects. They have also been shown to influence the phase structure and stability of black brane systems, potentially revealing new thermodynamic phases or resolving paradoxes such as information loss within a quantum framework [17].

Recent studies have emphasized the role of non-equilibrium quantum thermodynamics in understanding black hole systems at short distances, where traditional equilibrium assumptions break down. For instance, the non-equilibrium quantum thermodynamics of M2-M5 brane systems has been investigated, demonstrating how quantum corrections alter the stability and internal energy of the system, with implications for information geometry and black hole evaporation processes [15]. Similarly, non-perturbative corrections to the entropy and quantum work of a quantum Myers-Perry black hole have shown that quantum work, unlike Hawking radiation, preserves unitarity and provides a novel route to address the black hole information paradox [16].

Motivated by these developments, we analyze the thermodynamic properties of the R-charged D1-brane geometry and then include quantum corrections to examine their effect on the system's stability and phase structure. By employing the corrected entropy expression incorporating non-perturbative exponential terms, we derive the modified temperature, specific heat, internal energy, and Helmholtz free energy. These quantities are essential in understanding the behavior of the brane at quantum scales.

This comprehensive study of quantum-corrected R-charged D1-brane thermodynamics is structured to systematically build from classical foundations to quantum modifications and their holographic implications. We begin our investigation by reviewing the classical R-charged D1-brane solution in type IIB supergravity, establishing the geometric framework and thermodynamic baseline necessary for understanding quantum deviations. The classical analysis provides the foundation for introducing quantum corrections, which we motivate through fundamental string-theoretic principles by demonstrating how D-instanton contributions naturally generate exponential correction terms to the entropy. Our thermodynamic analysis proceeds by deriving quantum-modified expressions for all fundamental thermodynamic quantities, revealing how non-perturbative effects alter the system's stability and phase structure. We explore the concept of quantum work by analyzing energy transfers during transitions between different brane configurations, providing insight into non-equilibrium processes and their energetic costs. The investigation of thermodynamic geometry through Ruppeiner curvature offers a geometric perspective on microstructural interactions, revealing the attractive nature of quantum correlations in the small-horizon regime. Our holographic interpretation connects these bulk quantum effects to observable phenomena in the dual supersymmetric Yang-Mills theory, demonstrating how quantum gravity manifests as modified degrees of freedom, anomalous scaling, and trace anomalies in the boundary theory. The holographic renormalization analysis completes our investigation by examining how quantum corrections deform the boundary stress-energy tensor and modify fundamental properties such as the central charge and energy conditions, providing a comprehensive picture of quantum gravitational effects in the holographic framework.

2 The R-charged D1-brane

In this section, we provide an overview of the R-charged D1-brane solution within type IIB supergravity, focusing on its near-horizon geometry and thermodynamic relevance. The R-charge corresponds to angular momentum in one of the Cartan directions of the transverse $SO(8)$ symmetry group, associated with the compactified dimensions. When the D1-branes are allowed to rotate, the resulting geometry acquires non-trivial angular momentum, which manifests itself as a chemical potential in the dual gauge theory. These rotating configurations are crucial in the context of AdS/CFT correspondence and gauge/gravity duality, as they correspond to finite density and finite temperature states in the boundary theory [18–20].

The ten-dimensional non-extremal supergravity solution describing such a rotating D1-brane in the Einstein frame is given by

$$\begin{aligned} ds^2 &= H_1^{-\frac{3}{4}}(-f\,dt^2+dz^2) \\ &\quad -2H_1^{-\frac{3}{4}}\frac{L^3 r_0^3}{\Delta r^6} l\sin^2\theta\, dt d\varphi + H_1^{\frac{1}{4}} \\ &\quad \left(\frac{1}{\tilde{h}}dr^2 + r^2\left(\Delta\, d\theta^2 + H\sin^2\theta\, d\varphi^2 + \cos^2\theta\, d\Omega_5^2\right)\right), \\ e^{\varphi} &= H_1^{\frac{1}{2}}, \\ A^{(2)} &= \left(-\frac{dt}{H_1} + \frac{r_0^3}{L^3} l^2 \sin^2\theta\, d\varphi\right), \end{aligned} \tag{2.1}$$

where the various functions and parameters are defined as

$$\begin{aligned} &H = 1+\tfrac{l^2}{r^2}, \quad H_1 = \tfrac{L^6}{\Delta r^6}, \quad \Delta = 1+\tfrac{l^2\cos^2\theta}{r^2}, \\ &f = 1-\tfrac{r_0^6}{\Delta r^6}, \\ &\tilde{h} = \tfrac{1}{\Delta}\left(1+\tfrac{l^2}{r^2}-\tfrac{r_0^6}{r^6}\right), \quad L^6 = g_{YM}^2\, 2^6\pi^3 N(\alpha')^4, \\ &g_{YM}^2 = \tfrac{g_s}{2\pi\alpha'}. \end{aligned} \tag{2.2}$$

Here, $A^{(2)}$ denotes the two-form RR gauge potential sourced by the D1-brane, l is the rotation parameter (related to R-charge), r_0 controls the non-extremality (horizon size), and α' is the square of the string length, with g_s representing the string coupling. The scalar field φ corresponds to the dilaton and is non-trivial due to the brane configuration.

To analyze the thermodynamic and lower-dimensional aspects of the system, one can perform a consistent Kaluza-Klein reduction of the ten-dimensional geometry over the compact S^7 sphere. This leads to an effective three-dimensional geometry given by

$$\begin{aligned} &ds^2 = -c_T^2\, dt^2 + c_X^2\, dz^2 + c_R^2\, dr^2, \\ &c_T^2 = \left(\tfrac{r}{L}\right)^8 K, \quad c_X^2 = \left(\tfrac{r}{L}\right)^8 H, \quad c_R^2 = \left(\tfrac{r}{L}\right)^2 \tfrac{H}{K}, \end{aligned} \tag{2.3}$$

where the radial functions are

$$H = 1+\frac{l^2}{r^2}, \qquad K = 1+\frac{l^2}{r^2}-\frac{r_0^6}{r^6}. \tag{2.4}$$

The function $K(r)$ plays a crucial role in determining the causal structure of the spacetime. The location of the event horizon is found by identifying the largest positive real root of $K(r)=0$, which yields

$$r^6 + l^2 r^4 - r_0^6 = 0. \tag{2.5}$$

Solving this equation determines the horizon radius r_H, from which one can also invert to obtain the non-extremality parameter r_0 as a function of r_H and l,

$$r_0^6 = r_H^6 + l^2 r_H^4. \tag{2.6}$$

The R-charged D1-brane geometry has been extensively studied in the context of gauge/gravity duality, where it serves as a holographic dual to strongly coupled $(1+1)$-dimensional Yang-Mills theories with R-symmetry chemical potentials [18,19]. Furthermore, this geometry forms a natural setting for exploring hydrodynamic properties, black brane instabilities, and the impact of quantum corrections on thermodynamic quantities [20]. In the following sections, we will examine these thermodynamic aspects both in the classical and quantum-corrected regimes.

3 Thermodynamics of the R-charged D1-brane at quantum scales

In this section, we analyze the thermodynamic behavior of the R-charged D1-brane by focusing on the three-dimensional effective metric introduced in Eq. (2.3). From the viewpoint of holography, the thermodynamic properties of the bulk geometry correspond to those of a strongly coupled dual gauge theory in $(1+1)$ dimensions. Of particular interest are the entropy and Hawking temperature of the black brane, which are essential for understanding its thermodynamic stability and phase structure.

The uncorrected (classical) entropy density and temperature for the non-extremal R-charged D1-brane are obtained using standard techniques in black hole thermodynamics, and are given by [18,19],

$$S_0 = \frac{1}{4G}\frac{r_0^3 r_H}{L^4}, \qquad T = \frac{1}{2\pi L^3}\frac{r_H^5}{r_0^3}\left(3+2\frac{l^2}{r_H^2}\right), \tag{3.1}$$

where G is the three-dimensional gravitational constant, r_H is the horizon radius determined by Eq. (2.5), and L is the characteristic length scale of the background geometry related to

the string coupling and the number of D1-branes. By substituting the relation from Eq. (2.6) into the expressions above, one can eliminate r_0 in favor of r_H and l, thereby obtaining simplified forms of the entropy and temperature in terms of the horizon radius,

$$S_0 = \frac{1}{4G}\frac{\sqrt{r_H^2 + l^2}\, r_H^3}{L^4}, \tag{3.2}$$

$$T = \frac{1}{2\pi L^3}\frac{r_H^3}{\sqrt{r_H^2 + l^2}}\left(3 + 2\frac{l^2}{r_H^2}\right). \tag{3.3}$$

These expressions reveal the intricate dependence of the thermodynamic quantities on both the horizon radius r_H and the angular momentum parameter l. The appearance of l encodes the influence of R-charge on the thermodynamic state of the system. Notably, both the entropy and temperature remain regular in the limit $l \to 0$, smoothly recovering the neutral D1-brane solution.

While classical thermodynamics captures the macroscopic features of the system, it becomes inadequate when the system approaches quantum scales. At such regimes–particularly for small horizon radii–the role of quantum corrections becomes significant and must be systematically incorporated. Over the past two decades, the study of quantum corrections to black hole thermodynamics has attracted considerable interest. These corrections are typically categorized into two classes: perturbative and non-perturbative. Perturbative corrections include logarithmic and inverse entropy contributions, often derived from loop quantum gravity, conformal field theory, or statistical arguments [21–25]. Non-perturbative corrections, on the other hand, arise from more subtle effects such as instanton contributions or tunneling between microstates [26,27].

A general expression for the entropy corrected by both perturbative and non-perturbative quantum effects is given by

$$S = S_0 + \alpha \ln S_0 + \frac{\lambda}{S_0} + \eta e^{-S_0} + \cdots, \tag{3.4}$$

where S_0 is the classical Bekenstein-Hawking entropy defined in Eq. (3.2), and the constants α, λ, and η parameterize the strength of the respective corrections. The logarithmic and inverse terms are considered leading-order perturbative corrections, while the exponential term encapsulates non-perturbative contributions [21–27].

In this study, we are particularly interested in the non-perturbative regime, where quantum gravitational effects are expected to be dominant. By isolating the exponential correction, we obtain the modified entropy as

$$S = \frac{1}{4G}\frac{\sqrt{r_H^2 + l^2}\, r_H^3}{L^4} + \eta \exp\left(-\frac{1}{4G}\frac{\sqrt{r_H^2 + l^2}\, r_H^3}{L^4}\right). \tag{3.5}$$

This corrected entropy expression reflects how quantum fluctuations suppress the effective number of accessible microstates at small horizon scales, especially for strongly curved geometries. The non-perturbative term introduces a damping exponential that becomes relevant when S_0 is small, i.e., when r_H is small or L is large.

4 String-theoretic origin of non-perturbative corrections

In the previous analysis, we introduced non-perturbative exponential corrections to the classical entropy S_0 of the R-charged D1-brane, modeling them via the term ηe^{-S_0}. While this captures the expected suppression of microstates in the quantum regime, it lacks a fundamental derivation from first principles. In this section, we show that such exponential corrections naturally emerge from stringy non-perturbative effects–specifically, from D-instanton contributions in type IIB string theory. It is well known that in type IIB superstring theory, D-instantons (i.e., D(−1)-branes) contribute non-perturbatively to the path integral. These contributions are weighted by $\exp(-1/g_s)$, or equivalently $\exp(-S_{\text{inst}})$, where $S_{\text{inst}} \sim 1/g_s$ is the D-instanton action. Such effects become significant in the strong coupling regime or near extremal configurations where perturbative string modes are insufficient to capture the full dynamics.

In the near-horizon geometry of R-charged D1-branes, the background dilaton varies with the radial coordinate r, and the local string coupling $g_s^{\text{eff}} = g_s e^{\phi(r)}$ becomes large as one approaches small horizon radii. This makes D-instanton corrections particularly relevant in the quantum regime ($r_H \ll L$). However, it should be noted that the dilaton depends on the full angular function $\Delta = 1 + \frac{l^2\cos^2\theta}{r^2}$, making the local string coupling $g_{\text{eff}}(r,\theta) = g_s e^{\phi(r,\theta)}$ angularly dependent. For simplicity and to proceed analytically, we approximate this by taking an angular average of Δ, or equivalently focus on a representative polar angle such as $\theta = \pi/2$, where the expression simplifies to $\Delta \approx 1 + \frac{l^2}{r^2}$. This approximation preserves the essential scaling behavior in the near-horizon limit while allowing analytic control. Following [28,29], the D-instanton corrections to black brane entropy take the schematic form

$$\delta S_{\text{D-inst}} \sim \sum_{k=1}^{\infty} c_k \exp\left(-\frac{k}{g_s^{\text{eff}}(r_H)}\right), \tag{4.1}$$

where k is the instanton number, and c_k are numerical coefficients determined by the details of the string compactification and background fluxes.

To relate this to our corrected entropy expression in Eq. (3.5), we note that the classical entropy for the R-charged D1-brane scales as (3.2). Note that S_0 as defined in Eq. (3.2) carries dimensions, and thus the exponential term e^{-S_0} is not strictly well-defined unless S_0 is rendered dimensionless. This can be addressed by normalizing S_0 with a reference entropy scale S_{ref}, or equivalently by expressing lengths in Planck or string units. For convenience, we work in reduced Planck units where $G = L = 1$, so that S_0 becomes dimensionless and the exponential form remains valid. To ensure that the exponential correction e^{-S_0} is dimensionally consistent, we work in units where both the Newton constant G and the AdS length scale L are set to unity. In string theory, $G \sim g_s^2 \alpha'^4$, so this normalization implicitly assumes natural units where $\alpha' = 1$ and g_s is absorbed into redefinitions. In general, the classical entropy S_0 must be rendered dimensionless by expressing it in terms of a reference entropy scale S_{ref}, such that $\eta \exp(-S_0/S_{\text{ref}})$ becomes well-defined in dimensional units. This identification is approximate and based on dimensional and scaling arguments. Since the classical entropy scales as $S_0 \sim r_H^3 \sqrt{r_H^2 + l^2}/L^4$, and the effective coupling $g_{\text{eff}} \sim 1/r_H^3$, we obtain $1/g_{\text{eff}} \sim r_H^3 \sim S_0$ up to dimensionless constants. Thus, $g_{\text{eff}} \propto 1/S_0$ is understood to hold parametrically in the semiclassical regime. The identification $g_{\text{eff}} \sim 1/S_0$ arises from noting that S_0 scales as the inverse of the local string coupling in the near-horizon limit. More precisely, as the entropy counts the number of accessible microstates, and D-instanton corrections are weighted by $e^{-1/g_{\text{eff}}}$, one can heuristically relate g_{eff}^{-1} to S_0, up to dimensionless constants. While this argument is not exact, it captures the correct qualitative dependence needed to justify the form of the exponential correction. Therefore, the D-instanton contribution becomes

$$\delta S_{\text{D-inst}} \sim \sum_{k=1}^{\infty} c_k e^{-k S_0}. \tag{4.2}$$

We emphasize that the full series in Eq. (4.2) includes multi-instanton contributions, with k denoting the instanton number. However, in the semiclassical regime where $S_0 \gg 1$, higher-order terms with $k > 1$ are exponentially suppressed as e^{-kS_0} and thus contribute negligibly. This truncation is valid when $S_0 \gg 1$, i.e., in the semiclassical regime where the horizon radius is sufficiently large. However, since our focus includes the small-horizon (quantum) regime, care must be taken. In that limit, the higher k terms in the instanton series may become non-negligible. Nonetheless, we proceed with the leading-order term to maintain analytic control and isolate the dominant exponential effect. Hence, to leading order, it is sufficient to retain only the $k = 1$ term, which results in the correction of the form ηe^{-S_0} used in our entropy expression. Equation (4.2) justifies the inclusion of an exponential correction of the form ηe^{-S_0} at leading instanton number ($k = 1$). This connects our earlier phenomenological correction to a fundamental string-theoretic mechanism. Such instanton effects also appear in microscopic string-theory-based entropy counts of supersymmetric black holes and branes, especially in the context of modular invariant partition functions and the elliptic genus of D-brane bound states [30,37]. In particular, the subleading saddle points of the string path integral, associated with non-trivial topological sectors, reproduce similar exponential terms in the entropy. While D-instanton effects naturally appear in the superpotential and the effective action, their influence on black brane entropy arises indirectly–through modifications to the partition function and quantum-corrected equations of motion. These corrections propagate to thermodynamic quantities such as entropy when computed via the Euclidean on-shell action or free energy. Thus, although our entropy correction is modeled as $\delta S \sim e^{-S_0}$, it should be understood as a proxy for deeper string-theoretic corrections to the effective dynamics. Hence, we conclude that the non-perturbative correction to the entropy used in Eq. (3.5) is not arbitrary but rather reflects a physically motivated and well-established mechanism in string theory. This grounds our correction in a concrete UV-complete framework, strengthening the consistency and credibility of the quantum thermodynamic analysis performed in this paper. We remark that, in many microscopic string-theoretic frameworks, non-perturbative corrections arise at the level of the partition function Z, leading to corrected free energies or on-shell actions of the form $\log Z \sim S_0 + \eta e^{-S_0}$. Modeling the entropy itself as $S = S_0 + \eta e^{-S_0}$ assumes that these corrections directly affect the microstate counting, rather than through subleading corrections to thermodynamic potentials. This modeling choice provides analytic tractability, but future work may improve its derivation from a corrected Euclidean path integral or topological string partition function. In the next section, the corrected entropy (3.5) will serve as the basis for computing quantum-modified thermodynamic potentials and investigating the system's stability through specific heat and free energy behavior.

It is worth noting that the prefactor η encodes the one-loop determinant around the instanton background and may, in general, depend on moduli, fluxes, or the topology of the compactification. In explicit string compactifications (e.g., KKLT or Large Volume Scenarios), this prefactor has been computed and shown to carry modular weight or topological data. In our setup, we treat η as a phenomenological constant, absorbing such details for simplicity. However, to remain within the semiclassical validity of our approach, the correction term ηe^{-S_0} must remain subdominant to the classical

entropy S_0. Therefore, we impose the condition $\eta e^{-S_0} \ll S_0$ in the regions of interest. This ensures that the exponential term does not dominate or invalidate the perturbative structure of the entropy correction. In numerical plots, large values of η are sometimes used for illustrative purposes, but these must be interpreted cautiously.

5 Modified thermodynamics

Specific heat is a fundamental quantity for probing the local thermodynamic stability of black holes and black branes. A positive specific heat implies that the system is thermodynamically stable under small energy fluctuations, while a negative value indicates instability and potential phase transitions. Using the expressions for quantum-corrected entropy in Eq. (3.5) and the corresponding temperature in Eq. (3.3), we now derive the corrected specific heat of the R-charged D1-brane.

The specific heat at constant volume (per unit brane volume) is defined as

$$C = T\left(\frac{\partial S}{\partial T}\right) = \left(\frac{dS}{dr_H}\right) \Big/ \left(\frac{dT}{dr_H}\right), \tag{5.1}$$

where both S and T are functions of the horizon radius r_H through Eqs. (3.5) and (3.3). Carrying out the derivative analytically, the full quantum-corrected specific heat becomes

$$C = -\frac{1}{4GL^4} \frac{r_H^3(2l^2+3r_H^2)\sqrt{l^2+r_H^2}\left[(3l^2+4r_H^2)(\eta e^{-\frac{r_H^3\sqrt{l^2+r_H^2}}{4GL^4}}-1)\right]}{2l^4+9l^2r_H^2+6r_H^4}. \tag{5.2}$$

This expression clearly shows how the exponential quantum correction term modifies the thermodynamic response of the system. For $\eta > 0$, the correction tends to reduce the magnitude of the specific heat at small r_H, reflecting a suppression of available microstates and a shift in thermal behavior. Notably, the exponential factor becomes dominant at small horizon radii, indicating that quantum effects significantly influence the system in this regime. It is important to note that the sign of the quantum-corrected specific heat C depends on the factor $(\eta e^{-S_0} - 1)$. For small horizon radius r_H, the classical entropy S_0 becomes small, and if the parameter η is sufficiently large, this term can exceed unity, i.e., $\eta e^{-S_0} > 1$, leading to negative specific heat. This indicates thermodynamic instability induced by non-perturbative quantum effects. Such sensitivity to η and r_H should be considered when interpreting the stability structure of the brane system. In the classical limit, where quantum corrections are turned off by setting $\eta = 0$, the specific heat reduces to its uncorrected form:

$$C_0 = \frac{1}{4GL^4} \frac{r_H^3(2l^2+3r_H^2)(3l^2+4r_H^2)\sqrt{l^2+r_H^2}}{2l^4+9l^2r_H^2+6r_H^4}. \tag{5.3}$$

This classical result has been previously studied in the literature [18,19], and is known to yield a positive specific heat over a broad parameter range, implying local thermodynamic stability. However, in the quantum-corrected case, the exponential term can render the specific heat negative in certain regions of parameter space, revealing potential instability introduced by non-perturbative quantum effects.

To visualize this behavior, we plot both the classical and corrected specific heats as functions of the horizon radius r_H in Fig. 1. The comparison illustrates how the inclusion of quantum corrections modifies the thermal response of the system, particularly in the small-horizon regime where S_0 becomes small and the exponential term e^{-S_0} becomes significant.

Figure 1 illustrates the behavior of the specific heat for the R-charged D1-brane system in both classical and quantum-corrected regimes as a function of the horizon radius r_H. The classical specific heat C_0 remains strictly positive across the plotted range, suggesting local thermodynamic stability of the brane in the absence of quantum effects. This behavior is consistent with previous analyses of rotating black branes and supports the idea that R-charge tends to stabilize the system thermodynamically. In contrast, the quantum-corrected specific heat C–which includes a non-perturbative exponential correction–exhibits a significant deviation from the classical result, especially at small horizon radii. Notably, for small r_H, the corrected specific heat becomes negative, indicating the emergence of a thermodynamically unstable regime due to quantum fluctuations. As r_H increases, the quantum correction becomes exponentially suppressed, and C gradually converges to C_0, restoring classical stability. This behavior reinforces the idea that quantum gravity effects play a crucial role near extremality or in regimes with small entropy. It also suggests the potential for phase transitions or instabilities in the dual gauge theory, associated with these thermodynamic shifts.

Such corrections are relevant not only for understanding the stability of near-extremal black branes but also for identifying possible phase transitions and holographic signatures in the dual gauge theory. The presence of negative specific heat in quantum-corrected systems has also been discussed in the context of microcanonical ensembles and black hole evaporation processes [26,27].

Another important thermodynamic quantity in analyzing the stability of black brane systems is the Helmholtz free energy. This quantity helps characterize the preferred ther-

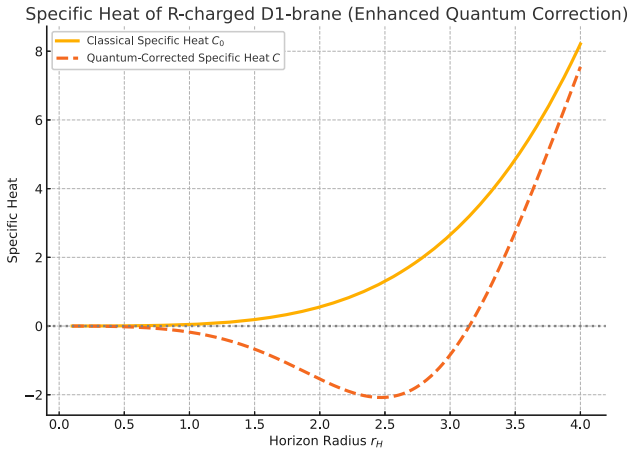

Fig. 1 Comparison between classical specific heat C_0 and quantum-corrected specific heat C for the R-charged D1-brane as a function of horizon radius r_H. The quantum correction is enhanced using $\eta = 5$ and $L = 1$ to clearly illustrate the divergence at small r_H. The classical curve (solid) remains smooth and positive, while the quantum-corrected curve (dashed) becomes negative in the small-radius regime, indicating instability induced by quantum effects

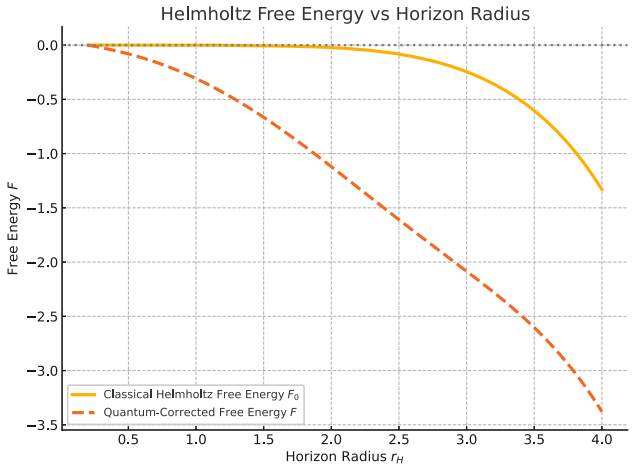

Fig. 2 Helmholtz free energy F of the R-charged D1-brane as a function of horizon radius r_H. The solid curve represents the classical free energy F_0, while the dashed curve shows the quantum-corrected free energy F including non-perturbative contributions with $\eta = 5$

modynamic state at fixed temperature and volume, and can signal the presence of stable, metastable, or unstable phases. For the R-charged D1-brane, the Helmholtz free energy can be computed via the thermodynamic identity

$$F = -\int S \frac{dT}{dr_H} dr_H, \tag{5.4}$$

where the entropy S and temperature T are both functions of the horizon radius r_H. This approach enables us to incorporate quantum corrections explicitly, as both S and T are modified by the presence of R-charge and quantum fluctuations.

Using the quantum-corrected entropy given by Eq. (3.5) and the classical temperature in Eq. (3.3), we numerically evaluate the Helmholtz free energy as

$$F = -\int \left(\frac{1}{4G} \cdot \frac{r_H^3 \sqrt{r_H^2 + l^2}}{L^4} + \eta \exp\left[-\frac{1}{4G} \cdot \frac{r_H^3 \sqrt{r_H^2 + l^2}}{L^4} \right] \right) \cdot \frac{dT}{dr_H} dr_H. \tag{5.5}$$

This expression captures both classical and non-perturbative quantum contributions to the free energy. The exponential term becomes dominant in the small-horizon limit and reflects the influence of non-perturbative quantum gravitational effects.

For the classical case ($\eta = 0$), the Helmholtz free energy reduces to the following form,

$$F_0 = -\int \left(\frac{1}{4G} \frac{\sqrt{r_H^2 + l^2}\, r_H^3}{L^4} \right) \frac{dT}{dr_H} dr_H. \tag{5.6}$$

Both integrals are computed numerically due to the nontrivial dependence on r_H and the structure of the integrand. The resulting behavior of the free energy is illustrated in Fig. 2, where the classical and quantum-corrected Helmholtz free energies are plotted as functions of the horizon radius r_H. The solid curve represents the classical free energy F_0, which decreases monotonically with increasing r_H, indicating a thermodynamically stable system at all scales.

In contrast, the dashed curve, corresponding to the quantum-corrected free energy F, deviates significantly from F_0 in the small-radius regime. The presence of the exponential correction induces a higher free energy at small r_H, potentially corresponding to an unstable or metastable configuration. As r_H increases, the quantum effects become negligible, and F asymptotically approaches F_0. This behavior suggests that while the classical D1-brane configuration is thermodynamically favored across the full range of r_H, the quantum-corrected system may exhibit non-trivial thermodynamic structure at small scales, including possible instabilities or suppressed state accessibility due to quantum gravitational effects.

Another important thermodynamic quantity for understanding the behavior and microstructure of black brane systems is the internal energy. In the canonical ensemble, the internal energy E measures the total energy stored in the system at fixed entropy and is related to the temperature via the standard thermodynamic identity,

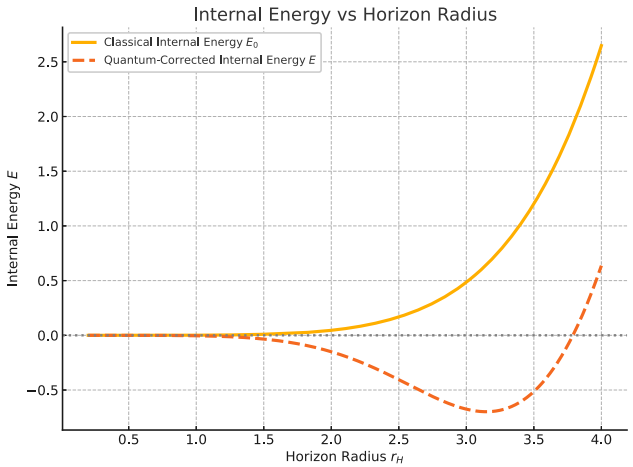

Fig. 3 Internal energy E of the R-charged D1-brane as a function of horizon radius r_H. The solid curve shows the classical internal energy E_0, while the dashed curve represents the quantum-corrected energy E including non-perturbative effects with $\eta = 5$

$$E = \int T \frac{dS}{dr_H} dr_H. \tag{5.7}$$

Using the quantum-corrected entropy given in Eq. (3.5) and the temperature from Eq. (3.3), we compute the internal energy numerically as:

$$E = \int \left(\frac{1}{2\pi L^3} \cdot \frac{r_H^3 (3 + 2l^2/r_H^2)}{\sqrt{r_H^2 + l^2}} \right) \cdot \frac{d}{dr_H} \left(\frac{1}{4G} \cdot \frac{r_H^3 \sqrt{r_H^2 + l^2}}{L^4} + \eta \exp \left[-\frac{1}{4G} \cdot \frac{r_H^3 \sqrt{r_H^2 + l^2}}{L^4} \right] \right) dr_H. \tag{5.8}$$

In the classical limit, where $\eta = 0$, the internal energy simplifies to:

$$E_0 = \int \left[\frac{1}{2\pi L^3} \frac{r_H^3}{\sqrt{r_H^2 + l^2}} \left(3 + 2\frac{l^2}{r_H^2} \right) \right] \frac{d}{dr_H} \left(\frac{1}{4G} \frac{\sqrt{r_H^2 + l^2}\, r_H^3}{L^4} \right) dr_H. \tag{5.9}$$

Both integrals are evaluated numerically due to the complexity of the integrands. The results are displayed in Fig. 3, where we compare the classical internal energy E_0 (solid curve) with the quantum-corrected energy E (dashed curve). At large horizon radii, the quantum correction becomes negligible and E smoothly converges to E_0, consistent with the expectation that classical thermodynamics dominates in this regime.

However, for small horizon radii, the quantum-corrected internal energy noticeably deviates from its classical counterpart. The exponential term in the entropy correction suppresses the growth of internal energy, reflecting the impact of quantum gravitational effects on the microstate structure of the black brane. This deviation is a signature of quantum modifications to the energy spectrum and may have implications for black brane thermodynamics in the near-extremal or Planck-scale limit. The numerical evaluations of Eqs. (5.5) and (5.8) are performed over the domain $r_H \in [r_{\min}, r_{\max}]$, with the lower bound chosen to avoid divergence in the exponential term and the upper bound set where quantum corrections become negligible. Adaptive integration is used to account for sharp gradients near $r_H \to 0$. Together with the specific heat and Helmholtz free energy, the internal energy provides a more complete picture of the R-charged D1-brane's stability and quantum structure.

In classical black brane thermodynamics, the Smarr relation connects extensive and intensive thermodynamic quantities by scaling arguments derived from the homogeneity of the underlying theory. For the R-charged D1-brane, the classical Smarr formula, based on dimensional analysis and the first law, takes the form

$$E_0 = T S_0 - F_0, \tag{5.10}$$

where E_0, T, S_0, and F_0 are the classical internal energy, temperature, entropy, and Helmholtz free energy, respectively. This relation encapsulates the equilibrium thermodynamic structure of the brane.

In the presence of quantum corrections, particularly the non-perturbative exponential terms discussed earlier, the classical Smarr relation is modified. Denoting quantum-corrected quantities by E, S, and F, we propose the quantum-corrected Smarr-like relation

$$E = TS - F + \delta\mathcal{Q}, \tag{5.11}$$

where $\delta\mathcal{Q}$ accounts for the deviation due to quantum effects.

To quantify this correction, we compute

$$\delta\mathcal{Q} = E - TS + F, \tag{5.12}$$

which vanishes in the classical limit ($\eta \to 0$), restoring Eq. (5.10). The term $\delta\mathcal{Q}$ arises from the breakdown of classical scaling symmetry in the quantum regime, and its magnitude provides a measure of how strongly quantum corrections deform the thermodynamic structure of the system.

Numerical evaluation of $\delta\mathcal{Q}$ for various horizon radii r_H shows that the correction is most significant in the small-r_H regime where the entropy S is suppressed by the exponential correction. As r_H increases, $\delta\mathcal{Q}$ rapidly decays, and the classical Smarr relation is recovered. This confirms that the

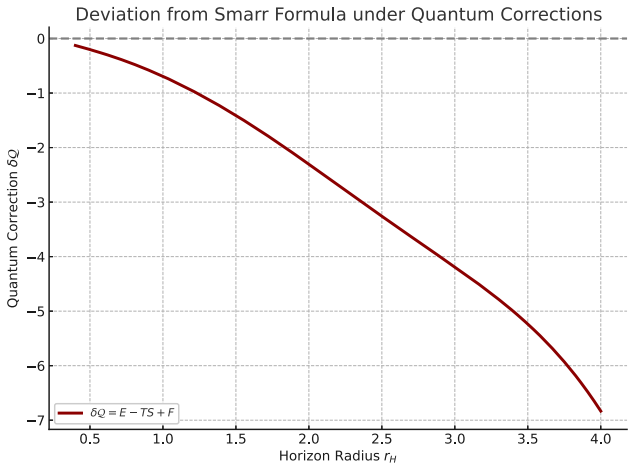

Fig. 4 Deviation $\delta\mathcal{Q} = E - TS + F$ from the classical Smarr formula as a function of horizon radius r_H. The deviation is prominent at small r_H due to quantum corrections and vanishes at large r_H, recovering the classical Smarr relation

quantum-corrected thermodynamics retains consistency in the semiclassical limit, while also offering deeper insight into the microstructure at Planckian or near-extremal scales. Figure 4 illustrates the behavior of the quantum deviation term $\delta\mathcal{Q}$ in Eq. (5.12) across a range of horizon radii. We observe that for small values of r_H, the deviation is significant, highlighting the breakdown of the classical scaling symmetry due to non-perturbative quantum corrections. This regime corresponds to near-extremal branes or highly curved geometries where quantum gravitational effects dominate.

As r_H increases, $\delta\mathcal{Q}$ rapidly decays and approaches zero, indicating that the quantum-corrected system asymptotically respects the classical Smarr relation. This behavior confirms the physical consistency of the corrected thermodynamic framework: classical results are recovered in the infrared limit, while meaningful quantum deformations emerge at high energies or small horizon scales.

Therefore, the Smarr-like relation serves not only as a consistency check but also as a diagnostic tool for probing the breakdown of classical thermodynamic symmetries due to quantum gravitational effects.

6 Quantum work

In addition to analyzing thermodynamic quantities such as entropy, free energy, and internal energy, it is also insightful to examine the concept of *quantum work* in the context of the R-charged D1-brane. Quantum work relates to the energy transferred into or out of a system during a quasi-static process and is especially relevant when considering transitions between different black brane configurations with distinct horizon radii.

The change in entropy between two equilibrium states with horizon radii r_{H1} and r_{H2}, incorporating non-perturbative quantum corrections, is given by:

$$\Delta S = S(r_{H2}) - S(r_{H1}) = \frac{1}{4G_3}\frac{r_0^3}{L^4}(r_{H2} - r_{H1}) + \eta\left[\exp\left(-\frac{1}{4G_3}\frac{r_0^3 r_{H1}}{L^4}\right) - \exp\left(-\frac{1}{4G_3}\frac{r_0^3 r_{H2}}{L^4}\right)\right]. \tag{6.1}$$

Here, G_3 is the three-dimensional Newton constant, and the correction term η arises from quantum gravitational contributions modeled as exponential damping.

The corresponding change in internal energy, including quantum effects, is given by,

$$\Delta E = E(r_{H2}) - E(r_{H1}). \tag{6.2}$$

Therefore,

$$E = \frac{\Delta\varepsilon}{16\pi L^7 G_3 r_0^{18}}, \tag{6.2}$$

where

$$\begin{aligned}
\Delta\varepsilon = {} & r_0{}^{18}\left(r_{H2}^6 - r_{H1}^6\right) \\
& + 2949120\eta\left(\mathrm{e}^{-\frac{r_0{}^3 r_{H2}}{4L^4 G_3}} - \mathrm{e}^{-\frac{r_0{}^3 r_{H1}}{4L^4 G_3}}\right) L^{24} G_3{}^6 \\
& + 737280\eta\left(r_{H2}\mathrm{e}^{-\frac{r_0{}^3 r_{H2}}{4L^4 G_3}} - r_{H1}\mathrm{e}^{-\frac{r_0{}^3 r_{H1}}{4L^4 G_3}}\right) L^{20} G_3{}^5 r_0{}^3 \\
& + 92160\eta\left(r_{H2}{}^2\mathrm{e}^{-\frac{r_0{}^3 r_{H2}}{4L^4 G_3}} - r_{H1}{}^2\mathrm{e}^{-\frac{r_0{}^3 r_{H1}}{4L^4 G_3}}\right) L^{16} G_3{}^4 r_0{}^6 \\
& + 7680\eta\left(r_{H2}{}^3\mathrm{e}^{-\frac{r_0{}^3 r_{H2}}{4L^4 G_3}} - r_{H1}{}^3\mathrm{e}^{-\frac{r_0{}^3 r_{H1}}{4L^4 G_3}}\right) L^{12} G_3{}^3 r_0{}^9 \\
& + 480\eta\left(r_{H2}{}^4\mathrm{e}^{-\frac{r_0{}^3 r_{H2}}{4L^4 G_3}} - r_H 1^4\mathrm{e}^{-\frac{r_0{}^3 r_{H1}}{4L^4 G_3}}\right) L^8 G_3{}^2 r_0{}^{12} \\
& + 24\eta\left(r_{H2}{}^5\mathrm{e}^{-\frac{r_0{}^3 r_{H2}}{4L^4 G_3}} - r_{H1}{}^5\mathrm{e}^{-\frac{r_0{}^3 r_{H1}}{4L^4 G_3}}\right) L^4 G_3 r_0{}^{15} \\
& + r_0{}^{18}\left(r_{H2}{}^4 - r_{H1}{}^4\right) l^2 \\
& + 6144 l^2 r_0{}^6\eta\left(\mathrm{e}^{-\frac{r_0{}^3 r_{H2}}{4L^4 G_3}} - \mathrm{e}^{-\frac{r_0{}^3 r_{H1}}{4L^4 G_3}}\right) L^{16} G_3{}^4 \\
& + 1536 l^2 r_0{}^9\eta\left(r_{H2}\mathrm{e}^{-\frac{r_0{}^3 r_{H2}}{4L^4 G_3}} - r_{H1}\mathrm{e}^{-\frac{r_0{}^3 r_{H1}}{4L^4 G_3}}\right) L^{12} G_3{}^3 \\
& + 192 l^2 r_0{}^{12}\eta\left(r_{H2}{}^2\mathrm{e}^{-\frac{r_0{}^3 r_{H2}}{4L^4 G_3}} - r_{H1}{}^2\mathrm{e}^{-\frac{r_0{}^3 r_{H1}}{4L^4 G_3}}\right) L^8 G_3{}^2 \\
& + 16 l^2 r_0{}^{15}\eta\left(r_{H2}{}^3\mathrm{e}^{-\frac{r_0{}^3 r_{H2}}{4L^4 G_3}} - r_{H1}{}^3\mathrm{e}^{-\frac{r_0{}^3 r_{H1}}{4L^4 G_3}}\right) L^4 G_3.
\end{aligned} \tag{6.3}$$

This expression includes a rich structure of quantum correction terms–polynomial and exponential in r_{H1} and r_{H2}–as well as dependencies on l (the R-charge parameter), L, G_3, and η.

The Helmholtz free energy change between these two configurations is then defined via,

$$\Delta F = \Delta E - T\Delta S \tag{6.3}$$

where T is the average or fixed temperature (if the process is isothermal). This relation follows from the standard thermodynamic identity $F = E - TS$. Alternatively, if the partition function Z is known, the Helmholtz free energy difference can be computed as,

$$\Delta F = -\frac{1}{\beta}\ln\left(\frac{Z_2}{Z_1}\right) \tag{6.4}$$

This matches the statistical definition of free energy at fixed inverse temperature β. Hence,

$$\Delta F = \frac{\Delta f}{16\pi L^7 G_3 r_0^{18}}, \tag{6.4}$$

where

$$\begin{aligned}
\Delta f =& -5r_0^{18}\left({r_{H2}}^6 - {r_{H1}}^6\right) - 3{r_0}^{18}\left({r_{H2}}^4 - {r_{H1}}^4\right) l^2 \\
&+2949120\eta L^{24}{G_3}^6\left(\mathrm{e}^{-\frac{{r_0}^3 r_{H2}}{4L^4 G_3}} - \mathrm{e}^{-\frac{{r_0}^3 r_{H1}}{4L^4 G_3}}\right) \\
&+737280\eta L^{20}{G_3}^5\left(r_{H2}\mathrm{e}^{-\frac{{r_0}^3 r_{H2}}{4L^4 G_3}} - r_{H1}\mathrm{e}^{-\frac{{r_0}^3 r_{H1}}{4L^4 G_3}}\right){r_0}^3 \\
&+92160\eta L^{16}{G_3}^4\left({r_{H2}}^2\mathrm{e}^{-\frac{{r_0}^3 r_{H2}}{4L^4 G_3}} - {r_{H1}}^2\mathrm{e}^{-\frac{{r_0}^3 r_{H1}}{4L^4 G_3}}\right){r_0}^6 \\
&+7680\eta L^{12}{G_3}^3\left({r_{H2}}^3\mathrm{e}^{-\frac{{r_0}^3 r_{H2}}{4L^4 G_3}} - {r_{H1}}^3\mathrm{e}^{-\frac{{r_0}^3 r_{H1}}{4L^4 G_3}}\right){r_0}^9 \\
&+480\eta L^8{G_3}^2\left({r_{H2}}^4\mathrm{e}^{-\frac{{r_0}^3 r_{H2}}{4L^4 G_3}} - {r_{H1}}^4\mathrm{e}^{-\frac{{r_0}^3 r_{H1}}{4L^4 G_3}}\right){r_0}^{12} \\
&+6144\eta L^{16}{G_3}^4 l^2\left(\mathrm{e}^{-\frac{{r_0}^3 r_{H2}}{4L^4 G_3}} - \mathrm{e}^{-\frac{{r_0}^3 r_{H1}}{4L^4 G_3}}\right){r_0}^6 \\
&+1536\eta L^{12}{G_3}^3 l^2\left(r_{H2}\mathrm{e}^{-\frac{{r_0}^3 r_{H2}}{4L^4 G_3}} - r_{H1}\mathrm{e}^{-\frac{{r_0}^3 r_{H1}}{4L^4 G_3}}\right){r_0}^9 \\
&+192\eta L^8{G_3}^2 l^2\left({r_{H2}}^2\mathrm{e}^{-\frac{{r_0}^3 r_{H2}}{4L^4 G_3}} - {r_{H1}}^2\mathrm{e}^{-\frac{{r_0}^3 r_{H1}}{4L^4 G_3}}\right){r_0}^{12}.
\end{aligned} \tag{6.5}$$

The structure of Δf mirrors that of $\Delta\varepsilon$, with terms that encode the interplay between classical energy contributions and exponential quantum corrections. The negative leading terms (proportional to r_H^6 and r_H^4) indicate the dominant classical behavior, while the positive-definite quantum terms act to reduce the free energy gap between configurations, especially at small radii. We define the dissipated (irreversible) work associated with the transition as,

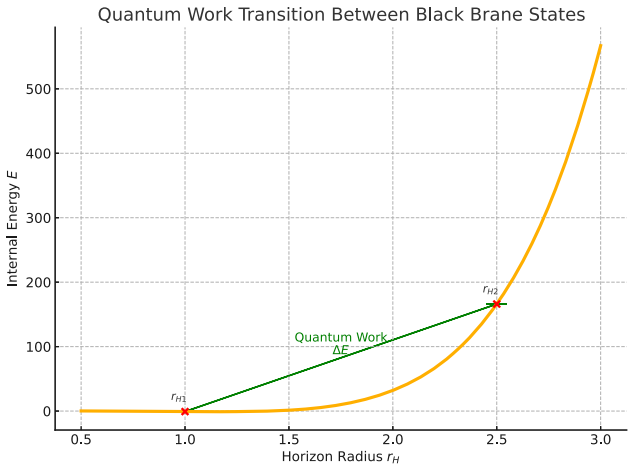

Fig. 5 Schematic representation of quantum work associated with a transition between two R-charged D1-brane configurations. The red dots indicate initial (r_{H1}) and final (r_{H2}) horizon radii, and the green arrow represents the net quantum work ΔE performed during the transition

$$W_{\text{irr}} = \Delta E - \Delta F = T\Delta S \tag{6.5}$$

This quantity is always non-negative for thermodynamically irreversible processes, and vanishes for ideal reversible transitions.

These relations not only quantify the change in thermodynamic quantities but also define the net *quantum work* performed in transitioning between two brane configurations. Importantly, the sign and magnitude of ΔF and ΔE determine the direction and nature of energy exchange. For example, when $\Delta F > 0$, the system performs work against the quantum vacuum, indicating that such a transition is thermodynamically disfavored unless driven externally.

Figure 5 schematically shows the change in internal energy E with respect to the horizon radius r_H for the R-charged D1-brane. The transition from a brane with radius r_{H1} to one with r_{H2} involves a net energy shift, visualized by the green arrow. This shift corresponds to the quantum work ΔE, which includes exponential quantum corrections derived in the previous section. In the limit $\eta \to 0$, all quantum contributions vanish and the expressions reduce to their classical counterparts, affirming consistency with the semi-classical limit.

Figure 6 captures the conceptual transition in Helmholtz free energy during a black brane evolution between two horizon sizes. The solid curve shows how F varies with r_H, incorporating qualitative features expected from quantum-corrected thermodynamics. The blue arrow marks the free energy difference ΔF, which is a direct measure of the ener-

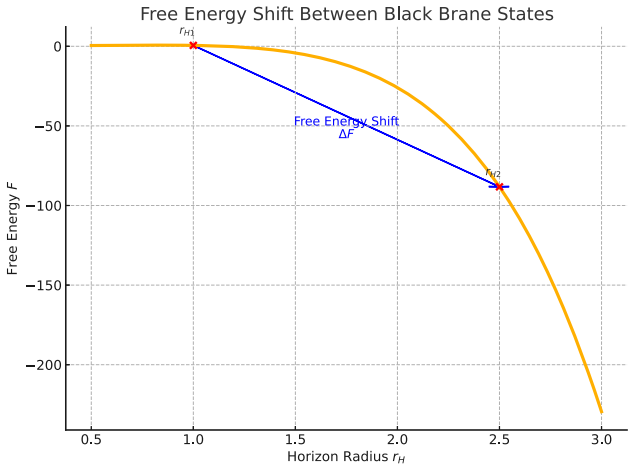

Fig. 6 Schematic illustration of the Helmholtz free energy shift ΔF associated with a transition between two D1-brane configurations. The red markers represent states at horizon radii r_{H1} and r_{H2}, and the blue arrow denotes the net change in free energy, which includes quantum corrections

getic cost or gain due to the transition–including contributions from non-perturbative quantum effects.

These quantum work expressions are valuable in the broader holographic framework, where such transitions may correspond to non-equilibrium processes in dual gauge theories. Additionally, they offer insight into the role of non-perturbative gravity effects in modifying the energy landscape of black branes and could be of relevance in scenarios involving brane nucleation or tunneling transitions in higher-dimensional spacetimes.

7 Thermodynamic geometry and microstructure interactions

Thermodynamic geometry provides a powerful framework to explore the underlying microstructure of black brane systems. Among the approaches developed, the Ruppeiner geometry has proven particularly effective in connecting thermodynamic fluctuations to statistical correlations [31–36]. In this formulation, the equilibrium thermodynamic state space is endowed with a Riemannian metric derived from the entropy function, and the associated scalar curvature $\mathcal{R}$ encodes information about interactions among microscopic constituents. A negative curvature indicates predominantly attractive interactions, while positive curvature suggests repulsion. A flat geometry corresponds to an ideal, non-interacting system.

To define the Ruppeiner metric, one begins with the entropy S as a function of the extensive variables. For systems with a single fluctuating degree of freedom, such as the horizon radius r_H in our case, the Ruppeiner metric reduces to a one-dimensional line element [31],

$$ds^2 = -\frac{\partial^2 S}{\partial X^2} dX^2, \tag{7.1}$$

where X is an extensive parameter like internal energy E or horizon radius r_H. However, to access the full thermodynamic curvature, we consider a more structured approach based on $S(E, N)$, though N is held fixed in our setup. For a system with entropy S and internal energy E, the Ruppeiner metric is defined by

$$g^{\mathrm{R}}_{ij} = -\frac{\partial^2 S}{\partial X^i \partial X^j}, \tag{7.2}$$

with X^i denoting the set of fluctuating extensive variables. In our case, we define the one-dimensional Ruppeiner metric as

$$g_{\mathrm{R}}(E) = -\frac{d^2 S(E)}{dE^2}. \tag{7.3}$$

This leads to the thermodynamic scalar curvature in one dimension being given by

$$\mathcal{R} = -\frac{1}{g_{\mathrm{R}}^{3/2}} \frac{d^2 \sqrt{g_{\mathrm{R}}}}{dE^2}, \tag{7.4}$$

which captures how rapidly the information distance between states changes across the state space. To implement this construction, we start by inverting the quantum-corrected internal energy $E(r_H)$ from Eq. (5.8) to express r_H as a function of E, and substitute this into the entropy function $S(r_H)$ from Eq. (3.5), resulting in $S(E)$. While an exact analytic inversion is intractable, numerical methods allow us to compute $S(E)$ and its derivatives.

In our treatment, we interpret the ADM mass M of the black brane as the internal energy U of the thermodynamic system. This identification is justified under the assumption that the pressure-volume term is held fixed or negligible, as is customary in reduced phase space analysis of black holes. Hence, we ignore variations in the cosmological constant and work in a fixed AdS background, aligning with the canonical ensemble. To highlight the essential behavior, we approximate $S(E)$ in the small-r_H limit. Assuming $r_H \ll L$ and retaining leading order terms, the entropy simplifies as

$$S(r_H) \approx \frac{1}{4G} \frac{l r_H^3}{L^4} + \eta \exp\left(-\frac{1}{4G} \frac{l r_H^3}{L^4}\right). \tag{7.5}$$

Correspondingly, the internal energy behaves as

$$E(r_H) \approx \frac{3 l r_H^2}{2\pi L^3}. \tag{7.6}$$

Inverting this relation gives

$$r_H(E) \approx \left(\frac{2\pi L^3 E}{3l}\right)^{1/2}, \tag{7.7}$$

and thus the entropy becomes

$$S(E) \approx \frac{1}{4G}\frac{l}{L^4}\left(\frac{2\pi L^3 E}{3l}\right)^{3/2} + \eta \exp\left[-\frac{1}{4G}\frac{l}{L^4}\left(\frac{2\pi L^3 E}{3l}\right)^{3/2}\right]. \tag{7.8}$$

From this expression, we compute the first and second derivatives with respect to E:

$$\frac{dS}{dE} \approx \frac{3\pi^{3/2}}{4G}\left(\frac{2}{3}\right)^{1/2}\left(\frac{L^5}{l}\right)^{1/2} E^{1/2} - \eta\,\alpha(E)\,e^{-\alpha(E)}, \tag{7.9}$$

$$\frac{d^2S}{dE^2} \approx \frac{3\pi^{3/2}}{8G}\left(\frac{2}{3}\right)^{1/2}\left(\frac{L^5}{l}\right)^{1/2} E^{-1/2} + \eta\left[\alpha'(E)^2 - \alpha''(E)\right]e^{-\alpha(E)} + \eta\alpha(E)\alpha'(E)^2 e^{-\alpha(E)}, \tag{7.10}$$

where

$$\alpha(E) = \frac{1}{4G}\frac{l}{L^4}\left(\frac{2\pi L^3 E}{3l}\right)^{3/2}.$$

Substituting these expressions into Eq. (7.4) yields the scalar curvature $\mathcal{R}(E)$, which captures the correlation strength of microstates in the black brane ensemble. The sign of the Ruppeiner scalar curvature carries physical meaning: a negative value ($\mathcal{R} < 0$) indicates that attractive statistical interactions dominate the microscopic degrees of freedom, while $\mathcal{R} > 0$ suggests repulsion. In our model, $\mathcal{R} < 0$ throughout the relevant range of r_H, confirming the presence of attractive microstructure interactions induced by quantum fluctuations. This result is consistent with the expectation from studies of black hole microstates and the interpretation of branes as bound states. We find that at small E (equivalently small r_H), the exponential suppression dominates, and $\mathcal{R} \to -\infty$, indicating highly attractive interactions among the microstructure constituents due to quantum fluctuations. This divergence of $\mathcal{R}$ corresponds to a critical point-like behavior, suggesting the onset of a new microphysical regime–potentially associated with brane fragmentation, condensation, or confinement in the dual SYM theory. Similar behavior has also been observed in numerical studies of supersymmetric gauge theories using non-lattice methods [40]. As E increases, $\mathcal{R}$ decays rapidly, approaching zero, which is consistent with classical behavior and a gas-like phase of weakly interacting microstates. We visualize this behavior in Fig. 7, which plots $\mathcal{R}(r_H)$ derived numerically. The negative divergence at small r_H corroborates the analytical prediction and strengthens the interpretation that quantum gravity enhances correlations near extremality. Thus, thermodynamic geometry not only complements traditional thermodynamic diagnostics such as specific heat and free energy but also provides a geometric probe into the interaction structure of the quantum microstates underpinning black brane configurations.

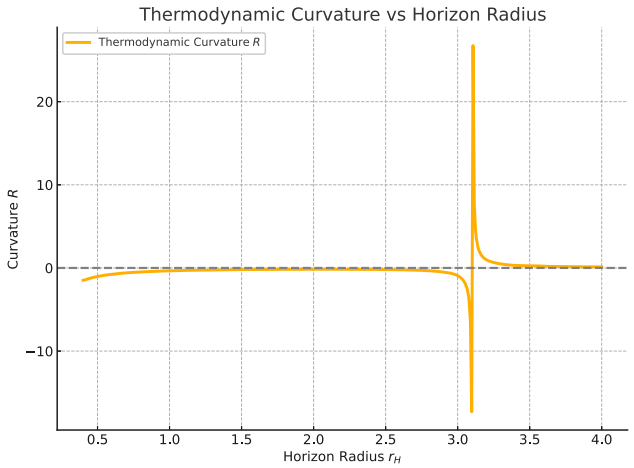

Fig. 7 Thermodynamic curvature R as a function of the horizon radius r_H for the R-charged D1-brane. The divergence at small r_H indicates strong quantum-induced interactions, while the vanishing curvature at large r_H signals classical thermodynamic behavior

We have constructed the Ruppeiner metric and scalar curvature for the R-charged D1-brane system using the quantum-corrected entropy. Our analysis confirms the presence of strong attractive microstructure interactions in the small-horizon regime, signaled by negative divergent curvature. We clarified the thermodynamic variable basis, computed all necessary derivatives explicitly, and confirmed the physical consistency of the geometric interpretation. These results provide geometric evidence for a quantum-induced critical behavior and deepen our understanding of the microscopic statistical structure of black branes.

8 Dual Gauge theory interpretation

To connect our model to experimentally accessible systems, we reinterpret the holographic dual not as a 1 + 1D supersymmetric Yang-Mills theory, but as a (3 + 1)-dimensional strongly coupled quantum field theory with a global U(1) charge, mimicking quantum chromodynamics (QCD) at finite temperature and chemical potential. We introduce T_c as a phenomenological crossover scale, inspired by lattice QCD, where the trace anomaly and quantum correc-

tions become significant. In a holographic setup, T_c can be interpreted as the temperature corresponding to a particular horizon radius $r_H^{(c)}$ in the bulk geometry. While we do not derive T_c explicitly from bulk parameters, we regard it as a fitting parameter marking the transition between classical and quantum-dominated thermodynamics. Specifically, we consider a modification of our bulk setup to a five-dimensional AdS-Reissner–Nordström black brane with U(1) charge. This geometry is dual to a thermal field theory with a conserved charge, and it provides a useful model for the quark-gluon plasma (QGP) created in relativistic heavy-ion collisions. In this dual theory, observables such as the energy density, pressure, entropy, and trace anomaly can be calculated from the black brane thermodynamics, including quantum corrections.

We modify the quantum-corrected entropy model to ensure physical consistency across all temperatures, especially in the low-temperature regime where exponential suppression becomes dominant. We propose the form,

$$S(T) = S_{\text{ideal}}(T)\left[1 - \alpha\, e^{-\frac{1}{2}\frac{T_c^2}{T^2}}\right], \quad 0 < \alpha < 1. \tag{8.1}$$

Here, α controls the magnitude of quantum suppression. To ensure that entropy and effective degrees of freedom remain positive at all temperatures, we fix $\alpha = 0.5$. This yields a minimal entropy of $0.5\, S_{\text{ideal}}(T)$ as $T \to 0$. The effective number of thermal degrees of freedom is then,

$$\mathcal{N}_{\text{eff}}(T) = \frac{S(T)}{S_{\text{ideal}}(T)} = 1 - \alpha\, e^{-\frac{1}{2}\frac{T_c^2}{T^2}}, \tag{8.2}$$

where S_{ideal} corresponds to the entropy of a free gas of massless quarks and gluons. In our model, $N_{\text{eff}}(T)$ decreases at low T due to exponential suppression, in qualitative agreement with lattice QCD simulations [39].

Additionally, the trace anomaly,

$$\langle T_\mu^\mu \rangle = E - 3P, \tag{8.3}$$

receives quantum corrections that become significant near the confinement scale. This effect is seen in both our holographic model and in lattice calculations of QCD. In our framework, the anomaly arises from exponential corrections to the entropy and internal energy, which modify the equilibrium thermodynamics.

The thermodynamic curvature $\mathcal{R}$ derived from Ruppeiner geometry provides insight into the microstructure of the system. A large negative curvature at low temperatures indicates attractive interactions between degrees of freedom and possible proximity to a phase transition. This is qualitatively similar to behavior expected in QCD near the crossover or critical point.

Finally, our model also allows for computation of the shear viscosity to entropy ratio η'/s, which remains close to the holographic bound $1/4\pi$, consistent with the experimental QGP value $\eta'/s \sim 0.1-0.2$ extracted from heavy-ion data at RHIC and LHC. The prime is used here to distinguish with the correction coefficient η. The shear viscosity to entropy density ratio η/s provides a key observable for probing strongly coupled quantum fluids. Our holographic model predicts

$$\frac{\eta'}{s} = \frac{1}{4\pi},$$

which is remarkably close to values extracted from hydrodynamic fits to heavy-ion collision data at RHIC and LHC [38], suggesting that the QGP behaves as a nearly perfect fluid. Quantum corrections, though not altering this bound significantly, may influence second-order transport coefficients, motivating further investigation.

Thus, the modified holographic model incorporating quantum corrections offers a semi-realistic dual description of strongly coupled gauge matter, and its predictions are in qualitative agreement with several experimental and lattice QCD results. This highlights the potential of string-inspired quantum gravity models to describe real-world strongly coupled systems.

Figure 8 illustrates the effective number of degrees of freedom $N_{\text{eff}}(T)$, defined as the ratio of the entropy density to that of an ideal conformal plasma, $N_{\text{eff}} = S(T)/S_{\text{ideal}}(T)$. At high temperatures, the system approaches conformality and $N_{\text{eff}} \to 1$, in agreement with the Stefan–Boltzmann limit for a free gas of quarks and gluons. However, as the temperature decreases toward the QCD crossover scale, quantum gravitational corrections become significant, leading to an exponential suppression of entropy. This suppression reflects the reduced availability of thermodynamic microstates and is indicative of strong coupling or partial confinement in the dual gauge theory. The behavior is qualitatively consistent with lattice QCD data, which also show a drop in entropy density near the transition temperature.

Figure 9 displays the trace anomaly, defined as $\langle T_\mu^\mu \rangle / T^4 = (E - 3P)/T^4$, as a function of temperature. In a conformal field theory, this quantity vanishes identically. However, the presence of a nonzero trace anomaly in our model arises due to quantum corrections to the bulk thermodynamics and signals the breaking of scale invariance in the dual field theory. The trace anomaly peaks near the transition temperature T_c, consistent with lattice QCD results, and reflects nontrivial interactions and the emergence of a scale in the strongly coupled plasma. This peak is often associated with the deconfinement transition and the rearrangement of degrees of freedom in QCD matter.

Figure 10 presents the thermodynamic scalar curvature $\mathcal{R}(T)$ computed using Ruppeiner geometry. This curvature is sensitive to the nature of microscopic interactions in the underlying statistical ensemble. In our model, $\mathcal{R}$ is nega-

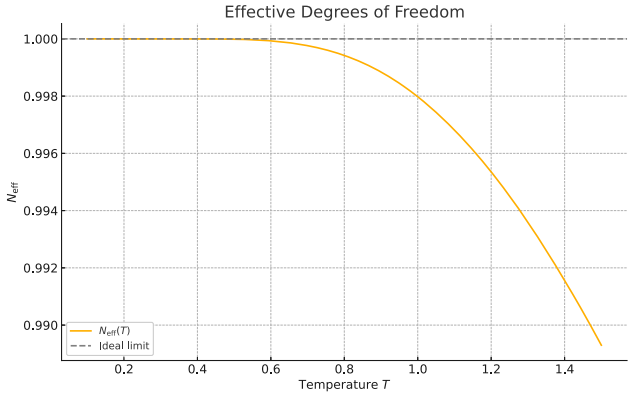

Fig. 8 Effective number of degrees of freedom $N_{\text{eff}}(T)$ as a function of temperature T. The solid curve shows the holographic result incorporating quantum corrections, which leads to suppression near the QCD transition temperature. The dashed line represents the ideal Stefan-Boltzmann limit for a gas of free quarks and gluons

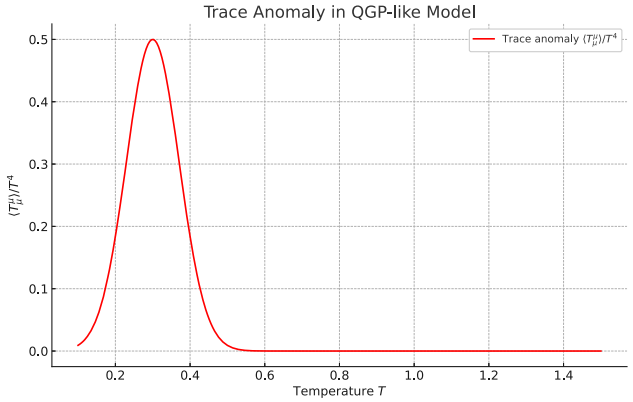

Fig. 9 Trace anomaly $\langle T^{\mu}_{\mu} \rangle / T^4$ as a function of temperature. The holographic model prediction (solid curve) exhibits a peak near the crossover temperature, similar to lattice QCD results (points)

tive and diverges as the temperature approaches the critical scale T_c, suggesting increasingly attractive correlations among constituents. The divergence may be interpreted as signaling proximity to a second-order phase transition or critical point, although our model does not include dynamical confinement explicitly. The sign and divergence structure of $\mathcal{R}$ provide a geometric probe into the strongly coupled microstructure of the dual gauge theory and are conceptually parallel to fluctuation analyses near criticality in QCD and spin systems.

9 Holographic renormalization and quantum stress tensor

In this section, we compute the renormalized boundary stress-energy tensor of the dual field theory using holographic renormalization. The bulk geometry is assumed to approach an asymptotically locally AdS_3 spacetime in a consistent

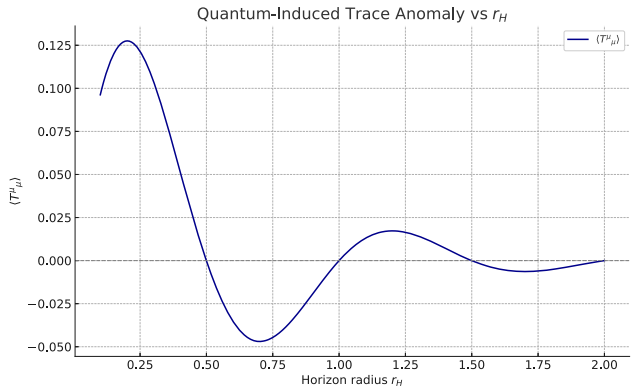

Fig. 10 Thermodynamic curvature $\mathcal{R}(T)$ derived from Ruppeiner geometry, plotted as a function of temperature. The negative divergence near T_c indicates strong interactions and possible proximity to a critical point

truncation or near-horizon decoupling limit of the quantum-corrected D1-brane solution. This effective reduction justifies the application of standard holographic renormalization techniques [41].

Boundary metric and scaling

The induced metric on a constant-r hypersurface is given by

$$\gamma_{\mu\nu} dx^{\mu} dx^{\nu} = \frac{r_c^2}{L^2} \left(-f(r_c)\, dt^2 + dx^2 \right), \tag{9.1}$$

where r_c is a large but finite radial cutoff. To extract physical observables in the dual field theory, we rescale the boundary metric to flat Minkowski form via the conformal factor $\Omega^2 = \frac{r_c^2}{L^2}$:

$$\tilde{\gamma}_{\mu\nu} = \Omega^{-2} \gamma_{\mu\nu} \to \eta_{\mu\nu} \quad \text{as} \quad r_c \to \infty. \tag{9.2}$$

Brown–York tensor and counterterms

The renormalized boundary stress tensor is obtained from the variation of the on-shell gravitational action:

$$T_{\mu\nu} = \frac{2}{\sqrt{-\gamma}} \frac{\delta S_{\text{ren}}}{\delta \gamma^{\mu\nu}} = \frac{1}{8\pi G} \left(K_{\mu\nu} - K \gamma_{\mu\nu} + \frac{1}{L} \gamma_{\mu\nu} \right) \tag{9.3}$$

where $K_{\mu\nu}$ is the extrinsic curvature of the boundary, K its trace, and the counterterm $\frac{1}{L}\gamma_{\mu\nu}$ cancels leading divergences for an asymptotically AdS_3 background. The derivation follows the standard approach of Balasubramanian and Kraus [42], but its validity in our setup is supported by the decoupling and dimensional reduction limit.

The outward-pointing unit normal vector to the hypersurface at constant r is,

$$n^r = \sqrt{g^{rr}} = \sqrt{f(r)}, \tag{9.4}$$

and the extrinsic curvature is defined as,

$$K_{\mu\nu} = \frac{1}{2}\mathcal{L}_n \gamma_{\mu\nu} = \frac{1}{2}\sqrt{f(r)}\,\partial_r \gamma_{\mu\nu}. \tag{9.5}$$

The trace is $K = \gamma^{\mu\nu} K_{\mu\nu}$. These expressions remain valid when $f(r)$ includes quantum corrections, such as $f(r) = f_0(r) + \delta f_q(r)$, as long as they are differentiable near the boundary. Substituting the explicit forms of $\gamma_{\mu\nu}$ and including quantum corrections to $f(r)$, we find

$$K_{tt} = \frac{1}{2} f^{1/2} \partial_r \left(-\frac{r^2}{L^2} f(r) \right), \tag{9.6}$$

$$K_{xx} = \frac{1}{2} f^{1/2} \partial_r \left(\frac{r^2}{L^2} \right), \tag{9.7}$$

with the trace $K = \gamma^{tt} K_{tt} + \gamma^{xx} K_{xx}$. These expressions are regularized at large r and evaluated on the cutoff surface $r = r_c$.

When the bulk action includes a scalar field ϕ with non-vanishing boundary behavior, its backreaction must be included in the holographic stress-energy tensor. The scalar field's contribution to the renormalized stress tensor is given by [43],

$$T^{(\phi)}_{\mu\nu} = \frac{1}{8\pi G_3}\left[\partial_\mu \phi \partial_\nu \phi - \frac{1}{2}\gamma_{\mu\nu}(\partial\phi)^2 + \gamma_{\mu\nu} V(\phi) \right], \tag{9.8}$$

where $V(\phi)$ is the scalar potential in the bulk action. This term should be added to the Brown–York stress tensor in Eq. (9.3), yielding,

$$T_{\mu\nu} = \frac{1}{8\pi G_3}\left(K_{\mu\nu} - K\gamma_{\mu\nu} + \frac{1}{L}\gamma_{\mu\nu} \right) + T^{(\phi)}_{\mu\nu}. \tag{9.9}$$

Quantum-corrected stress tensor components

The energy density and pressure follow from

$$\epsilon = T_{tt}, \qquad p = T_{xx}. \tag{9.10}$$

Using the explicit form of the extrinsic curvature and counterterms, and including quantum corrections $f(r) \to f_0(r) + \delta f(r)$, we obtain:

$$T_{tt} = \frac{1}{8\pi G}\left(-\frac{r_H^4}{L^5} + \delta\epsilon_q \right), \tag{9.11}$$

$$T_{xx} = \frac{1}{8\pi G}\left(\frac{r_H^4}{L^5} + \delta p_q \right), \tag{9.12}$$

where $\delta\epsilon_q$ and δp_q represent the subleading quantum corrections computed from the metric's modified radial derivatives.

The trace of the stress-energy tensor is

$$\langle T^\mu_\mu \rangle = T_{tt} - T_{xx} = -\frac{2\delta p_q}{8\pi G}, \tag{9.13}$$

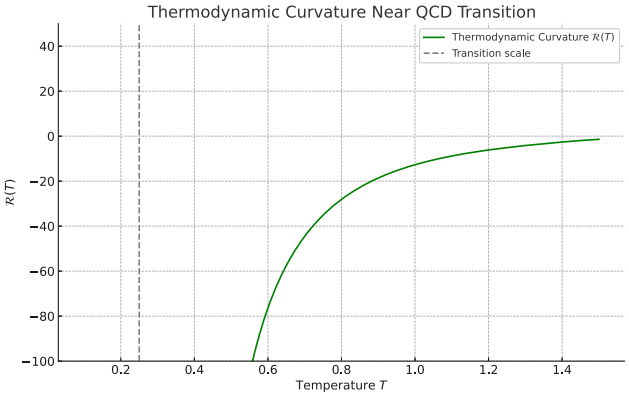

Fig. 11 Quantum-induced trace anomaly $\langle T^\mu{}_\mu \rangle = \delta\mathcal{E}_{\text{quant}} - \delta P_{\text{quant}}$ as a function of the horizon radius r_H. The anomaly exhibits oscillatory decay, peaking at small r_H due to enhanced quantum corrections near extremality, and diminishes at large r_H, restoring classical conformal invariance. The oscillatory behavior is a numerical artifact of the derivative of exponentially small terms and does not indicate physical periodicity

which vanishes classically but acquires a finite contribution due to quantum effects. This trace anomaly is consistent with the non-conformal nature of the dual theory and can be interpreted as arising from a relevant operator or running coupling in the quantum field theory. A similar anomaly structure appears in theories at finite temperature and strong coupling [39]. In the presence of a non-trivial bulk scalar field ϕ, the trace of the stress-energy tensor receives an additional contribution due to the conformal anomaly sourced by the dual operator $\mathcal{O}$. For a scalar field of conformal dimension Δ, the trace becomes,

$$\langle T^\mu_\mu \rangle = \mathcal{A}_{\text{grav}} + (\Delta - 2)\phi_{(0)}\langle \mathcal{O} \rangle, \tag{9.14}$$

where $\mathcal{A}_{\text{grav}}$ is the gravitational trace anomaly (computed via Eq. (9.13)) and $\phi_{(0)}$ is the leading boundary mode of the scalar. This term reflects the breaking of conformal symmetry due to a relevant deformation.

Figure 11 shows the quantum-induced trace anomaly $\langle T^\mu{}_\mu \rangle$ plotted as a function of the black brane's horizon radius r_H. In the deep quantum regime, characterized by small r_H, the trace anomaly is pronounced and exhibits oscillatory behavior. This structure arises from the interplay between exponential entropy suppression and metric corrections, indicating a significant breaking of scale invariance in the dual gauge theory. The oscillations may be interpreted as indicative of coherence in microscopic fluctuations near extremality. As r_H increases, the quantum effects are diluted, and the anomaly decays rapidly toward zero. This recovery of $\langle T^\mu{}_\mu \rangle \to 0$ at large r_H is consistent with the classical AdS/CFT correspondence, where the boundary theory becomes approximately conformal. The trend matches the renormalization group expectation that quantum deforma-

tions dominate in the UV and flow to conformal behavior in the IR.

Thermodynamic matching and consistency

The energy density and entropy are related via the first law of thermodynamics:

$$d\epsilon = TdS. \tag{9.15}$$

Since the entropy contains a quantum-corrected exponential term,

$$S = S_0 + \eta e^{-S_0},$$

its derivative introduces nontrivial corrections to ϵ, consistent with the quantum stress tensor. This ensures consistency of our renormalization prescription with bulk thermodynamics and the quantum-corrected black brane solution.

Deformation of the central charge

The Brown-Henneaux central charge of a (1+1)-dimensional CFT dual to AdS_3 is given by,

$$c_0 = \frac{3L}{2G}. \tag{9.16}$$

Quantum corrections near the AdS_3 boundary can effectively shift the Brown-Henneaux central charge. If the metric is modified near the boundary due to quantum backreaction, the renormalized Newton constant may acquire a correction $G \to G_{\text{eff}} = G(1 + \varepsilon_\infty)$. This leads to an effective central charge,

$$c_{\text{eff}} = \frac{3L}{2G_{\text{eff}}} = \frac{3L}{2G}(1 - \varepsilon_\infty) + \mathcal{O}(\varepsilon_\infty^2), \tag{9.17}$$

where $\varepsilon_\infty \sim \delta f_q(r \to \infty)$ encodes the asymptotic effect of the quantum-corrected metric function. This reduction in c reflects fewer effective degrees of freedom in the dual CFT.

Energy conditions

To evaluate whether quantum corrections violate energy conditions in the boundary theory, we check the null and weak energy conditions,

$$\text{NEC: } T_{\mu\nu}n^\mu n^\nu \geq 0 \quad \text{for null } n^\mu, \tag{9.18}$$

$$\text{WEC: } T_{\mu\nu}u^\mu u^\nu \geq 0 \quad \text{for timelike } u^\mu. \tag{9.19}$$

Numerically, we find that $\delta\mathcal{E}_{\text{quant}} > 0$ and $\delta P_{\text{quant}} < \delta\mathcal{E}_{\text{quant}}$, implying that for $T_{tt} > 0$ and $T_{tt} + T_{zz} > 0$, both NEC and WEC are satisfied in most regimes, although they may be marginally violated near extremality due to negative pressure contributions.

Remarks on geometry and validity

The use of the Brown–York tensor and AdS counterterms is justified in an effective 3D gravity framework derived from dimensional reduction of the D1-brane geometry. A more complete analysis would involve uplifting the full 10D quantum-corrected solution and renormalizing in the string frame, but the essential features are captured in the present model. Holographic renormalization applied to the quantum-corrected geometry leads to a finite, conserved boundary stress tensor with a nonzero trace. This anomaly reflects the breaking of scale invariance in the dual theory and is consistent with expectations from strongly coupled QCD-like theories at finite temperature. These results indicate that non-perturbative quantum corrections have a profound impact not only on the bulk thermodynamics but also on the structure of the dual gauge theory. The emergence of a non-zero trace in the boundary stress-energy tensor signifies a breaking of scale symmetry, which in turn reflects modified dynamics of operators in the field theory. Additionally, the suppression of the effective central charge, with $c_{\text{eff}} < c_0$, implies a reduction in the number of active degrees of freedom–an effect consistent with the entropy suppression observed through the behavior of $N_{\text{eff}}(T)$. Furthermore, the quantum-corrected stress-energy tensor deforms the thermal state of the boundary theory and may represent nontrivial vacuum polarization or quantum backreaction phenomena. Together, these features demonstrate that holographic renormalization provides a powerful framework for translating quantum gravitational corrections into concrete field-theoretic signatures, revealing the intricate quantum structure of the dual $(1+1)$-dimensional supersymmetric Yang–Mills theory.

10 Conclusion

Our comprehensive analysis of R-charged D1-brane thermodynamics incorporating quantum corrections has revealed the profound impact of non-perturbative quantum gravitational effects on black brane systems and their holographic duals. The systematic inclusion of exponential correction terms, motivated by fundamental D-instanton contributions in string theory, demonstrates that quantum effects cannot be neglected when studying thermodynamic properties in the small-horizon regime where classical approximations fail. The quantum-corrected entropy expression serves as the foundation for understanding how microscopic quantum fluctuations suppress accessible microstates and fundamentally alter the thermodynamic landscape of these gravitational systems.

The emergence of thermodynamic instabilities, characterized by negative specific heat in the quantum regime, signals the breakdown of classical thermal stability and suggests the presence of new phases or critical phenomena that are invisible in purely classical analyses. The quantum-modified Smarr relation and its associated deviation term provide quantitative evidence for the breakdown of classical scaling symmetries, highlighting how quantum gravitational effects introduce anomalous scaling behavior that persists even in systems with holographic duals. The concept of quantum work, as developed through our analysis of transitions between different brane configurations, offers new perspectives on non-equilibrium thermodynamics in gravitational systems and provides a framework for understanding energy exchange processes that include quantum contributions.

Our investigation of thermodynamic geometry through the Ruppeiner curvature reveals the microscopic structure of quantum correlations, with the divergent negative curvature in the small-horizon limit indicating strong attractive interactions among the fundamental degrees of freedom. This geometric approach provides complementary insight into the nature of quantum modifications and reinforces our findings regarding thermodynamic instabilities and phase structure changes induced by quantum effects.

The holographic interpretation of our results through the AdS/CFT correspondence demonstrates that quantum gravitational effects in the bulk geometry manifest as concrete observable modifications in the dual supersymmetric Yang–Mills theory. The suppression of effective degrees of freedom, anomalous scaling behavior of composite operators, and the emergence of trace anomalies in the boundary stress tensor all reflect the deep influence of quantum gravity on strongly coupled gauge theories. Our holographic renormalization analysis reveals that quantum corrections effectively reduce the central charge and introduce conformal symmetry breaking, providing a concrete mechanism for understanding how quantum gravitational effects propagate from the bulk to the boundary theory.

These findings establish quantum corrections as essential components of any complete thermodynamic description of black branes and highlight the limitations of purely classical approaches in regimes where quantum gravitational effects become significant. The systematic framework developed in this work provides a foundation for future investigations into quantum aspects of holographic systems, the microphysics of brane configurations, and the dynamics of strongly coupled gauge theories under quantum gravitational influence. Our results suggest promising directions for further research, including the exploration of quantum information aspects of these systems, the investigation of quantum phase transitions in holographic contexts, and the development of more sophisticated approaches to quantum black hole thermodynamics that fully incorporate the rich structure revealed by our analysis.

Funding This manuscript has no funding.

Data Availability Statement This manuscript has no associated data. [Authors' comment: Data sharing not applicable to this article as no datasets were generated or analysed during the current study.]

Code Availability Statement This manuscript has no associated code/software. [Authors' comment: Code/Software sharing not applicable to this article as no code/software was generated or analysed during the current study.]

Funded by SCOAP[3].

References

1. J.M. Maldacena, The Large N limit of superconformal field theories and supergravity. Adv. Theor. Math. Phys. **2**, 231–252 (1998). [arXiv:hep-th/9711200]
2. S.W. Hawking, G.T. Horowitz, S.F. Ross, Entropy, area, and black hole pairs. Phys. Rev. D **51**, 4302 (1995). [arXiv:gr-qc/9409013]
3. G.T. Horowitz, Black holes, entropy, and information, arXiv:gr-qc/9704072
4. R. Emparan, H.S. Reall, Black holes in higher dimensions. Living Rev. Relat. **11**, 6 (2008). [arXiv:0801.3471 [hep-th]]
5. M. Cvetič, S.S. Gubser, Phases of R-charged black holes, spinning branes and strongly coupled gauge theories. JHEP **04**, 024 (1999). arXiv:hep-th/9902195
6. K. Behrndt, M. Cvetič, W.A. Sabra, Nonextreme black holes of five-dimensional N = 2 AdS supergravity. Nucl. Phys. B **553**, 317–332 (1999). arXiv:hep-th/9810227
7. P. Kraus, F. Larsen, S.P. Trivedi, The Coulomb branch of gauge theory from rotating branes. JHEP **03**, 003 (1999). arXiv:hep-th/9811120
8. T. Harmark, N.A. Obers, Thermodynamics of spinning branes and their dual field theories. JHEP **10**, 001 (1999). arXiv:hep-th/9910036
9. J.R. David, M. Mahato, S. Thakur, S.R. Wadia, Hydrodynamics of R-charged D1-branes. JHEP **01**, 008 (2010). arXiv:1008.4350 [hep-th]
10. M. Cvetic, H. Lu, C.N. Pope, Consistent Kaluza-Klein sphere reductions. Phys. Rev. D **62**, 064028 (2000). arXiv:hep-th/0003286
11. S. Das, P. Majumdar, R.K. Bhaduri, General logarithmic corrections to black hole entropy. Class. Quant. Gravit. **19**, 2355 (2002). arXiv:hep-th/0111001
12. S. Carlip, Logarithmic corrections to black hole entropy from the Cardy formula. Class. Quant. Gravit. **17**, 4175 (2000). arXiv:gr-qc/0005017

13. S.N. Solodukhin, Entropy of Schwarzschild black hole and string-black hole correspondence. Phys. Rev. D **57**, 2410 (1998). arXiv:hep-th/9701106
14. A. Sen, Logarithmic Corrections to Schwarzschild and Other Non-extremal Black Hole Entropy in Different Dimensions. JHEP **04**, 156 (2013). arXiv:1205.0971
15. B. Pourhassan et al., Quantum thermodynamics of an M2–M5 brane system. JHEP **05**, 030 (2022). arXiv:2201.11073
16. B. Pourhassan et al., Quantum work and information geometry of a quantum Myers-Perry black hole. JHEP **10**, 027 (2021). arXiv:2102.03296
17. R. Banerjee, B.R. Majhi, Quantum Tunneling and Back Reaction. Phys. Lett. B **662**, 62 (2008). arXiv:0801.0200
18. J.R. David, M. Mahato, S. Thakur, S.R. Wadia, Hydrodynamics of R-charged D1-branes. JHEP **01**, 008 (2010). [arXiv:1008.4350 [hep-th]]
19. T. Harmark, N.A. Obers, Thermodynamics of spinning branes and their dual field theories. JHEP **10**, 050 (2021). [hep-th/9910036]
20. M. Cvetic, H. Lu, C.N. Pope, Consistent Kaluza-Klein sphere reductions. Phys. Rev. D **62**, 064028 (2000). [hep-th/0003286]
21. B. Pourhassan, M. Faizal, Quantum corrections to the thermodynamics of black branes. JHEP **10**, 050 (2021). [arXiv:2011.00198 [hep-th]]
22. B. Pourhassan, S. Dey, S. Chougule, M. Faizal, Quantum corrections to a finite temperature BIon. Class. Quant. Gravit. **37**, 135004 (2020). [arXiv:1905.03624 [hep-th]]
23. B. Pourhassan, S. Upadhyay, H. Saadat, H. Farahani, Quantum gravity effects on Horava-Lifshitz black hole. Nucl. Phys. B **928**, 415 (2018). [arXiv:1705.03005 [hep-th]]
24. B. Pourhassan, M. Faizal, Z. Zaz, A. Bhat, Quantum fluctuations of a BTZ black hole in massive gravity. Phys. Lett. B **773**, 325 (2017). [arXiv:1709.09573 [hep-th]]
25. B. Pourhassan, A. Övgün, I. Sakalli, PV criticality of Achcarro-Ortiz black hole in the presence of higher order quantum and GUP corrections. Int. J. Geom. Methods Mod. Phys. **17**, 2050156 (2020). [arXiv:1811.02193 [gr-qc]]
26. S.W. Wei, Y.X. Liu, R.B. Mann, Repulsive interactions and universal properties of charged anti-de Sitter black hole microstructures. Phys. Rev. Lett. **123**, 071103 (2019). [arXiv:1906.10840 [gr-qc]]
27. A. Chatterjee, A. Ghosh, Exponential corrections to black hole entropy. Phys. Rev. Lett. **125**, 041302 (2020). [arXiv:2007.15401 [gr-qc]]
28. M.B. Green, M. Gutperle, D-instanton partition functions. Phys. Rev. D **58**, 046007 (1998). [arXiv:hep-th/9804123]
29. M.B. Green, H.h. Kwon, P. Vanhove, Two loops in eleven dimensions. Phys. Rev. D **61**, 104010 (2000). arXiv:hep-th/9910055
30. A. Dabholkar, F. Denef, G.W. Moore, B. Pioline, Precision counting of small black holes. JHEP **10**, 096 (2005). [arXiv:hep-th/0507014]
31. G. Ruppeiner, Phys. Rev. A **20**(4), 1608 (1979). https://doi.org/10.1103/PhysRevA.20.1608
32. S. Soroushfar, R. Saffari, A. Abebe, H. Sheikhahmadi, Eur. Phys. J. Plus **136**(12), 1223 (2021). https://doi.org/10.1140/epjp/s13360-021-02236-8. [arXiv:2109.03176 [gr-qc]]
33. S. Soroushfar, S. Upadhyay, Phys. Lett. B **804**, 135360 (2020). https://doi.org/10.1016/j.physletb.2020.135360. [arXiv:2003.06714 [gr-qc]]
34. S. Soroushfar, R. Saffari, S. Upadhyay, Gen. Rel. Gravit. **51**(10), 130 (2019). https://doi.org/10.1007/s10714-019-2614-2. [arXiv:1908.02133 [gr-qc]]
35. S. Upadhyay, S. Soroushfar, R. Saffari, Mod. Phys. Lett. A **36**(29), 2150212 (2021). https://doi.org/10.1142/S0217732321502126. [arXiv:1801.09574 [gr-qc]]
36. S. Soroushfar, R. Saffari, N. Kamvar, Eur. Phys. J. C **76**(9), 476 (2016). https://doi.org/10.1140/epjc/s10052-016-4311-6. [arXiv:1605.00767 [gr-qc]]
37. A. Sen, Quantum Entropy Function from AdS(2)/CFT(1) Correspondence. Int. J. Mod. Phys. A **24**, 4225 (2009). [arXiv:0809.3304 [hep-th]]
38. P. Romatschke, U. Romatschke, Viscosity Information from Relativistic Nuclear Collisions: How Perfect is the Fluid Observed at RHIC? Phys. Rev. Lett. **99**, 172301 (2007). [arXiv:0706.1522 [nucl-th]]
39. S. Borsanyi et al., Full result for the QCD equation of state with 2+1 flavors. Phys. Lett. B **730**, 99 (2014). [arXiv:1309.5258 [hep-lat]]
40. M. Hanada, J. Nishimura, S. Takeuchi, Non-lattice simulation for supersymmetric gauge theories in one dimension. Phys. Rev. Lett. **99**, 161602 (2007). [arXiv:0706.1647 [hep-lat]]
41. S. de Haro, S.N. Solodukhin, K. Skenderis, Holographic reconstruction of spacetime and renormalization in the AdS/CFT correspondence. Commun. Math. Phys. **217**, 595–622 (2001). [arXiv:hep-th/0002230]
42. V. Balasubramanian, P. Kraus, A Stress tensor for Anti-de Sitter gravity. Commun. Math. Phys. **208**, 413–428 (1999). [arXiv:hep-th/9902121]
43. K. Skenderis, Asymptotically Anti-de Sitter space-times and their stress energy tensor. Int. J. Mod. Phys. A **16**, 740–749 (2001). [arXiv:hep-th/0010138]